

## ORIGINAL RESEARCH



# Microtubule-Mediated Regulation of $\beta_2$ AR Translation and Function in Failing Hearts

Zoe Kwan, Binoy Paulose Nadappuram<sup>1</sup>, Manton M. Leung<sup>1</sup>, Sanika Mohagaonkar<sup>1</sup>, Ao Li<sup>1</sup>, Kumuthu S. Amaradasa<sup>1</sup>, Ji Chen<sup>1</sup>, Stephen Rothery, Iyobel Kibreab, Jiarong Fu<sup>1</sup>, Jose L. Sanchez-Alonso<sup>1</sup>, Catherine A. Mansfield, Hariharan Subramanian, Alexander Kondrashov<sup>1</sup>, Peter T. Wright, Pamela Swiatlowska<sup>1</sup>, Viacheslav O. Nikolaev<sup>1</sup>, Beata Wojciak-Stothard, Aleksandar P. Ivanov<sup>1</sup>, Joshua B. Edel<sup>1</sup>, Julia Gorelik<sup>1</sup>

**BACKGROUND:**  $\beta_1$ AR (beta-1 adrenergic receptor) and  $\beta_2$ AR (beta-2 adrenergic receptor)-mediated cyclic adenosine monophosphate signaling has distinct effects on cardiac function and heart failure progression. However, the mechanism regulating spatial localization and functional compartmentation of cardiac  $\beta$ -ARs remains elusive. Emerging evidence suggests that microtubule-dependent trafficking of mRNP (messenger ribonucleoprotein) and localized protein translation modulates protein compartmentation in cardiomyocytes. We hypothesized that  $\beta$ -AR compartmentation in cardiomyocytes is accomplished by selective trafficking of its mRNAs and localized translation.

**METHODS:** The localization pattern of  $\beta$ -AR mRNA was investigated using single molecule fluorescence in situ hybridization and subcellular nanobiopsy in rat cardiomyocytes. The role of microtubule on  $\beta$ -AR mRNA localization was studied using vinblastine, and its effect on receptor localization and function was evaluated with immunofluorescent and high-throughput Förster resonance energy transfer microscopy. An mRNA protein co-detection assay identified plausible  $\beta$ -AR translation sites in cardiomyocytes. The mechanism by which  $\beta$ -AR mRNA is redistributed post-heart failure was elucidated by single molecule fluorescence in situ hybridization, nanobiopsy, and high-throughput Förster resonance energy transfer microscopy on 16 weeks post-myocardial infarction and detubulated cardiomyocytes.

**RESULTS:**  $\beta_1$ AR and  $\beta_2$ AR mRNAs show differential localization in cardiomyocytes, with  $\beta_1$ AR found in the perinuclear region and  $\beta_2$ AR showing diffuse distribution throughout the cell. Disruption of microtubules induces a shift of  $\beta_2$ AR transcripts toward the perinuclear region. The close proximity between  $\beta_2$ AR transcripts and translated proteins suggests that the translation process occurs in specialized, precisely defined cellular compartments. Redistribution of  $\beta_2$ AR transcripts is microtubule-dependent, as microtubule depolymerization markedly reduces the number of functional receptors on the membrane. In failing hearts, both  $\beta_1$ AR and  $\beta_2$ AR mRNAs are redistributed toward the cell periphery, similar to what is seen in cardiomyocytes undergoing drug-induced detubulation. This suggests that t-tubule remodeling contributes to  $\beta$ -AR mRNA redistribution and impaired  $\beta_2$ AR function in failing hearts.

**CONCLUSIONS:** Asymmetrical microtubule-dependent trafficking dictates differential  $\beta_1$ AR and  $\beta_2$ AR localization in healthy cardiomyocyte microtubules, underlying the distinctive compartmentation of the 2  $\beta$ -ARs on the plasma membrane. The localization pattern is altered post-myocardial infarction, resulting from transverse tubule remodeling, leading to distorted  $\beta_2$ AR-mediated cyclic adenosine monophosphate signaling.

**GRAPHIC ABSTRACT:** A [graphic abstract](#) is available for this article.

**Key Words:** animal ■ cardiomyocytes ■ heart failure ■ infarction ■ microtubules

Correspondence to: Julia Gorelik, PhD, Imperial College London, 429, 4th Floor, ICTEM Bldg, Hammersmith Campus, United Kingdom. W12 0BZ.

Email [j.gorelik@imperial.ac.uk](mailto:j.gorelik@imperial.ac.uk)

Supplemental Material is available at <https://www.ahajournals.org/doi/suppl/10.1161/CIRCRESAHA.123.323174>.

For Sources of Funding and Disclosures, see page 957.

© 2023 The Authors. *Circulation Research* is published on behalf of the American Heart Association, Inc., by Wolters Kluwer Health, Inc. This is an open access article under the terms of the [Creative Commons Attribution License](#), which permits use, distribution, and reproduction in any medium, provided that the original work is properly cited.

*Circulation Research* is available at [www.ahajournals.org/journal/res](http://www.ahajournals.org/journal/res)

## Novelty and Significance

### What Is Known?

- $\beta_1$ AR (beta-1 adrenergic receptor) and  $\beta_2$ AR (beta-2 adrenergic receptor) are functionally compartmentalized in cardiomyocytes.
- The mRNA for  $\beta_2$ AR contain specific structural elements for translational (inhibition) and mRNA localization control, whereas  $\beta_1$ AR mRNA does not. Some but not all mRNAs in cardiomyocytes are trafficked using the microtubule network.
- Heart failure alters cardiac function in several ways, including redistribution and dysregulation of  $\beta$ AR signaling.

### What New Information Does This Article Contribute?

- $\beta_2$ AR but not  $\beta_1$ AR mRNA is trafficked in cardiomyocytes using the microtubule network.
- $\beta_2$ AR protein localization and function at the plasma membrane compartment is regulated using the microtubule network.
- In failing cardiomyocytes,  $\beta_2$ AR mRNA is distributed differently than in normal myocytes.
- In heart failure, the dismantling of the transverse tubules (t-tubules) (detubulation) is a driving force leading to  $\beta_2$ AR redistribution, on both mRNA, protein and functional level.

Both  $\beta_1$ AR and  $\beta_2$ AR could be found on the plasma membrane of cardiomyocytes, with  $\beta_2$ AR predominantly compartmentalized to the t-tubules in healthy cardiomyocytes and  $\beta_1$ AR found throughout the sarcolemma membrane. In failing hearts,  $\beta_2$ AR redistributes from the t-tubules toward the sarcolemma membrane contributing to the loss in precise regulation of  $\beta_2$ AR-mediated cAMP signaling.

Using smFISH and nanoscale tweezer subcellular biopsy, we have discovered  $\beta_1$ AR and  $\beta_2$ AR mRNA distribute differently in cardiomyocytes, and that both mRNAs redistributed in failing hearts. Using a microtubule depolymerizing agent, we demonstrated on mRNA, protein, and functional levels that  $\beta_2$ AR but not  $\beta_1$ AR distribution is regulated by the microtubule network. When t-tubules were dismantled by a drug-induced acute detubulation, the loss of t-tubules lead to a physical redistribution of  $\beta_2$ AR.

Taken together, we have demonstrated the importance of  $\beta$ ARs localization in regulating proper cardiac function. By aiming to restore a proper structural landscape (t-tubules, microtubules), which will lead to a restoration of correct distribution of  $\beta$ 2AR on both mRNA and protein level, one could potentially restore the  $\beta_2$ AR-mediated cardiac function in failing hearts.

### Nonstandard Abbreviations and Acronyms

<b><math>\beta_1</math>AR</b>	beta-1 adrenergic receptor
<b><math>\beta_2</math>AR</b>	beta-1 adrenergic receptor
<b>ARVM</b>	adult rat ventricular myocyte
<b>cAMP</b>	cyclic adenosine monophosphate
<b>DI</b>	dispersion index
<b>FRET</b>	Förster resonance energy transfer
<b>HF</b>	heart failure
<b>mRNP</b>	messenger ribonucleoprotein
<b>PI</b>	polarization index
<b>smFISH</b>	single molecule fluorescence in situ hybridization
<b>t-tubule</b>	transverse tubule

**H**eat failure (HF) is one of the most common cardiac-related causes of death globally.<sup>1,2</sup> Cardiomyocytes, which comprise the bulk of the human heart, undergo various dynamic physiological changes during HF, such as distortion of the  $\beta$ -ARs ( $\beta$ -adrenergic receptors) signaling pathways. There are 3 types of  $\beta$ -ARs in the human myocardium, with  $\beta_1$ AR (beta-1 adrenergic receptor) and  $\beta_2$ AR (beta-2 adrenergic receptor) being

the 2 most abundant subtypes, existing at roughly 70:30 ratio.<sup>3–6</sup> Although  $\beta_1$ ARs and  $\beta_2$ ARs are highly similar in structure, they also have some distinctive features. For example, both  $\beta_1$ AR and  $\beta_2$ AR could trigger stimulatory Gas-protein activation, but the latter also can couple with inhibitory G $\alpha_i$ -protein making it possible for  $\beta_2$ AR to play multiple regulatory roles in mammalian hearts.<sup>7–11</sup> In failing hearts,  $\beta$ -AR signaling undergoes remodeling, a highly complex process, with features such as equalized expression and function between  $\beta_1$ AR and  $\beta_2$ AR (uncoupling from G proteins).<sup>12–14</sup>

Emerging evidence suggests that different  $\beta$ -AR subtypes modulate the downstream cyclic adenosine monophosphate (cAMP) signaling pathway differently, resulting in the differential compartmentation and signaling profile of the 2  $\beta$ -AR subtypes.<sup>15</sup> A 2010 study previously demonstrated that, unlike  $\beta_1$ AR, distributed throughout the plasma membrane,  $\beta_2$ AR is compartmentalized mainly to the transverse tubules (t-tubules) in healthy cardiomyocytes. However, this difference is lost in HF, where  $\beta_2$ ARs are physically redistributed from the t-tubules to the plasma membrane.<sup>16</sup> The mechanism of this redistribution remains unclear. What is known, however, is that t-tubule remodeling in cardiomyocytes is one of the hallmarks of HF and an indicator of the disease's progression.<sup>17–22</sup> In mammals, the  $\beta_1$ AR and  $\beta_2$ AR receptor proteins are encoded by the

Adrb1 and Adrb2 genes, respectively, both genes having no introns. Several studies highlighted the importance of regulation at the level of mRNA localization and protein synthesis for  $\beta_2$ AR. It has been demonstrated that Adrb2 mRNA, unlike Adrb1, can be initially translationally silent.<sup>18</sup> A 1994 study has shown that the 5' upstream open reading frame in the Adrb2 mRNA translates into a small peptide product that could inhibit the receptor's synthesis.<sup>23</sup> A more recent study has demonstrated that in DT1-MF2 and A431 cells, the binding of nucleocytoplasmic shuttling RNA-binding protein HuR to the 3'-UTR of Adrb2 mRNA is crucial in its translational silencing and trafficking to the cell membrane.<sup>24</sup> The authors showed that downregulation of HuR led to premature translational initiation of Adrb2 mRNA and mislocalization of the protein from the cell periphery to other subcellular locations,<sup>24</sup> highlighting the importance of mRNA trafficking for appropriate  $\beta_2$ AR receptor localization.

While one common mechanism of protein and signal compartmentation in some mammalian cells, such as neurons, is by localized protein translation,<sup>25,26</sup> it was previously unclear whether this applies to mammalian cardiomyocytes. However, in recent years, emerging evidence has demonstrated that at least some mRNAs in cardiomyocytes are locally translated into proteins in individual sarcomeres. In 2018, Lewis et al demonstrated for the first time that some sarcomeric proteins, including Myh6 (myosin heavy chain 6), are locally translated in individual sarcomeres. In addition, the authors found that many sarcomeric proteins are also locally degraded by ubiquitin.<sup>27</sup> Following that study, Scarborough et al<sup>28</sup> revealed that these sarcomeric factors were not the only transcripts found to be translated throughout mammalian cardiomyocytes, but in fact, it is a general phenomenon involving many transcripts in these cells. The mechanism for how mRNAs in mature mammalian cardiomyocytes are transported has also been suggested by the same study in which the microtubule network plays a key role.

Microtubules, a major component of the cell cytoskeleton, play a crucial role in intracellular trafficking in mammalian cells. Biological molecules such as mRNAs and proteins can be attached to microtubules as cargo complexes via motor proteins (eg, dynein), where multiple cargos can bind to multiple motor proteins of the same or opposite polarity.<sup>29–32</sup> In the 2021 study conducted by Scarborough et al,<sup>28</sup> the authors found that in adult rat ventricular myocytes (ARVMs), most mRNAs are trafficked using the microtubule network. The authors demonstrated that when the microtubule network was disrupted, mRNAs, rRNAs (translational machinery), and nascent protein products relocalized to the perinuclear region of ARVM, suggesting that an intact microtubule network is crucial to proper mRNA transportation in these cells for localized translation to take place, hence enabling proper localization of the translated proteins. A more recent study utilizing a highly sensitive and specific

fluorescent in situ hybridization (FISH) technique that can visualize 18s associated mRNAs of interest also demonstrated that in murine cardiomyocytes, some but not all mRNAs are locally translated into proteins.<sup>33</sup> It suggested that protein translation in cardiomyocytes can be conducted in different subcellular compartments and may be subject to remodeling upon local stimulation. Other than mRNP (messenger ribonucleoprotein) trafficking, the microtubule network has also been reported to be involved in regulating t-tubule stability in cardiomyocytes via anchoring proteins such as Junctophilin-2 and BIN1,<sup>34–37</sup> further indicating the importance of microtubule homeostasis in regulating normal cardiac function.

In this study, we aimed to investigate whether the compartmentation of  $\beta_2$ AR in cardiomyocytes is accomplished by selective trafficking of its mRNAs. We were also interested in finding out whether the localization pattern of  $\beta_2$ AR mRNA in failing cardiomyocytes changes and if this change is associated with the loss of compartmentation of the receptor protein on the plasma membrane. Since  $\beta_2$ AR mRNA has a unique feature where it is initially translationally repressed after nuclear export,<sup>24</sup> we hypothesized that localization of  $\beta_2$ ARs, but not  $\beta_1$ ARs, depends on local translation and hence proper mRNA trafficking in cardiomyocytes.

## METHODS

### Data Availability

Detailed methodology and protocols are included in the supplementary section.

## RESULTS

### A New Software for Clustering Analysis of smFISH Images on Multinucleated Cells

A clustering analysis approach for analyzing FISH images was reported by Hye et al utilizing the concept of polarization index (PI) and dispersion index (DI). Later, Stueland et al developed the original algorithm into software to automate the image analysis process.<sup>38</sup> The original algorithm was designed for analyzing single-nucleated cells, assuming the cell centroid and the nucleus centroid to be the same—which is the case for most single-nucleated cells. This is, however, not the case in ARVM, as these are binucleated cells. A new algorithm suitable for analyzing cells with multiple nuclei was therefore developed.

The geometric center of a cell, the nucleus, and the population of FISH signals in a particular digital image were each defined as a centroid (the averaged middle point of a particular cluster of fluorescent signals):

$$\text{Centroid} = \left( \frac{1}{n} \sum_i^n x_i, \frac{1}{n} \sum_i^n y_i \right) = (\bar{x}, \bar{y})$$

Where  $x$  and  $y$  are the pixel coordinates of the boundary of the cell, the nucleus, or the recognized FISH signals, and  $n$  is the number of points that define the cell boundary, the nucleus, and the FISH signals. To estimate the distribution of a given RNA cluster in relation to the cell size/shape across different cells, the radius of gyration (scalar) of the cell was first calculated using the cell mask.

$$\text{Radius of gyration } (Rg) = \sqrt{\frac{\sum_i^n \left[ \begin{array}{c} (x_i - \bar{x}_{\text{Cell}})^2 \\ + (y_i - \bar{y}_{\text{Cell}})^2 \end{array} \right]}{n}}$$

Where  $\bar{x}_{\text{Cell}}$ ,  $\bar{y}_{\text{Cell}}$  is the coordinates of the cell centroid,  $(x_i, y_i)$  is the collection of coordinates defining the cell boundary.

The displacement ( $d_0$ ) between the FISH signal cluster centroid and the nucleus centroid is described as the PI (Figure 1A). The longer the distance between the RNA signal cluster and the nucleus is, the greater the PI is. To compare the displacement across cells, we normalize the size of the displacement vector with the radius of the gyration of the cell. The cellular radius of gyration ( $Rg_{\text{Cell}}$ ) describes the cell morphology as a linear scalar to match the size of the displacement scalar.

$$\text{Polarisation Index } (PI) = \sqrt{\frac{\begin{array}{c} (\bar{x}_{\text{RNA}} - \bar{x}_{\text{Nucleus}})^2 \\ + (\bar{y}_{\text{RNA}} - \bar{y}_{\text{Nucleus}})^2 \end{array}}{Rg_{\text{cell}}}}$$

The DI was used to describe how tightly packed a given RNA cluster is. It summarizes the displacements between all RNA fluorescent signals and the RNA cluster centroid. The more dispersed the RNA signal, the higher the DI will be. As an intracellular component, RNA distribution is strongly influenced by the shape of the cell. The second moment of area of the RNA cluster and the cell was used to describe how fluorescent signals/points are distributed. The DI was expressed as the second moment of area of a given RNA cluster (the distribution of the RNA cluster) normalized to the second moment of area of the cell (the shape of the cell).

$$\text{Second moment}_{\text{RNA}} = \mu_2 = \frac{1}{n} \sum_i^n \left[ \begin{array}{c} (x_i - \bar{x}_{\text{RNA}})^2 \\ + (y_i - \bar{y}_{\text{RNA}})^2 \end{array} \right]$$

$$\text{Second moment}_{\text{Cell}} = \mu_2' = \frac{1}{m} \sum_i^m \left[ \begin{array}{c} (x_i - \bar{x}_{\text{Cell}})^2 \\ + (y_i - \bar{y}_{\text{Cell}})^2 \end{array} \right]$$

$$\text{Dispersion Index } (DI) = \frac{\mu_2}{\mu_2'}$$

Where  $\bar{x}_{\text{Cell}}$ ,  $\bar{y}_{\text{Cell}}$  is the coordinates of the cell centroid,  $(x_i, y_i)$  is the collection of coordinates defining the cell boundary.

In the case of multinucleated cells, the algorithm assumes that an individual RNA signal originated from its immediate nucleus. Therefore, within the same cell, each

RNA molecule signal is assigned to one of the 2 nuclei, and each nucleus will result in 2 indexes: 1 PI and 1 DI. The averaged PI/DI between all nuclei in that particular cell is used to represent the overall PI/ DI for that cell.

## Adrb1 and Adrb2 Are Differentially Localized in ARVM

To study the localization pattern of  $\beta_1$ AR or  $\beta_2$ AR mRNAs in ARVM, a dielectrophoretic (DEP) nanotweezer single-cell sampling technique was used.<sup>39</sup> These nanoscale tweezers generate an electric field gradient upon applying an alternating current across the 2 nanoelectrodes at their tip. This allows highly localized trapping and extraction of mRNA molecules from individual ARVMs. Highly localized single-cell biopsies (within 300 nm from the tweezer tip) were reproducibly obtained from the cell end, perinuclear region, and side edge of live adult rat cardiomyocytes in a highly precise manner (Figure 2A and 2B). TaqMan reverse transcription-quantitative PCR (RT-qPCR) analysis was used to detect and quantify the presence of  $\beta_1$ AR or  $\beta_2$ AR transcript in different cellular regions. The results revealed that most  $\beta$ -AR transcripts were found in the perinuclear regions regarding the subtype. However, some  $\beta_2$ ARs were also detected near the cell periphery (Figure 2C).

To confirm this finding, a highly sensitive and specific amplification-based Single molecule fluorescence in situ hybridization (smFISH) technology RNAscope was utilized. Qualitatively, it was revealed that  $\beta_1$ AR transcripts were found mainly in the perinuclear region, whereas  $\beta_2$ AR mRNAs were distributed throughout the cells (Figure 2D). Clustering analysis of the smFISH images showed  $\beta_1$ AR mRNA clustered around the nucleus with PIs and DIs of 0.088 and 0.111, respectively, whereas  $\beta_2$ AR mRNA distribution is more polarized and dispersed with PIs and DIs of 0.122 and 0.226, respectively (Figure 2E).

## An Intact Microtubule Network Is Essential in $\beta_2$ AR mRNA but Not $\beta_1$ AR mRNA Trafficking

To test whether the differential localization of the 2  $\beta$ -AR mRNAs is a result of spatially regulated mRNA trafficking via the microtubule network, we treated cardiomyocytes with 2  $\mu$ M vinblastine to disrupt the microtubule network in ARVM for 18 hours and observed its effect on  $\beta_1$ AR and  $\beta_2$ AR mRNAs localization. We have confirmed by immunostaining that treating ARVM with 2  $\mu$ M vinblastine for 18 hours sufficiently disrupted the microtubule network and that such treatment did not cause significant  $\beta_1$ AR and  $\beta_2$ AR gene expression alteration as confirmed by our RT-qPCR analysis on total extracted RNA (Figure S1).

After testing the efficacy of vinblastine in depolymerizing the microtubule network, we proceeded to extract nanobiopsy samples from the different cellular regions of

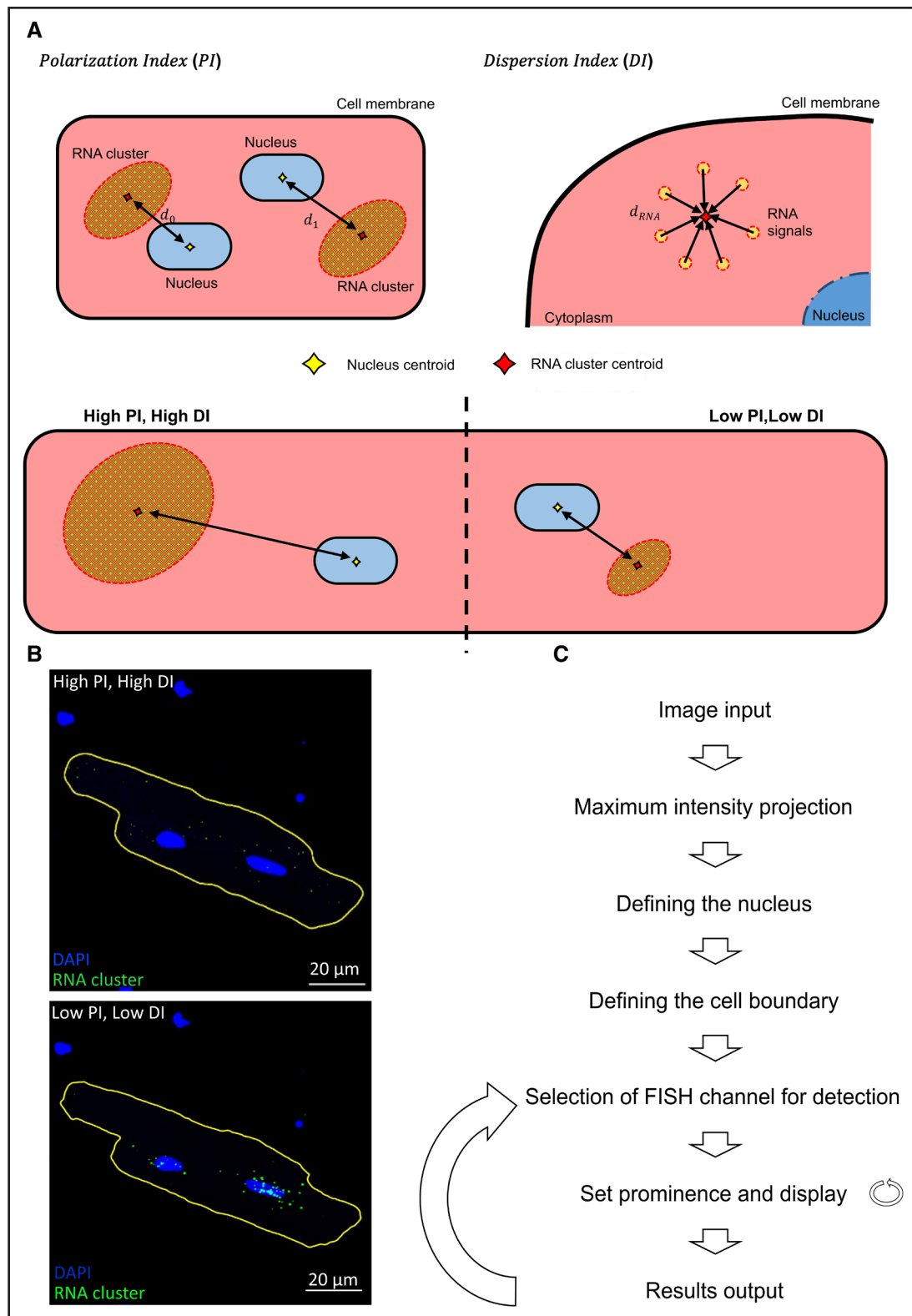


**Figure 1. Description of the algorithm used for understanding RNA distribution patterns in multinucleated cells by clustering analysis.**

**A**, Schematic of the concept of polarization index (PI) and dispersion index (DI). A high polarization index indicates a given RNA cluster traveled further away from the nucleus; a high dispersion index suggests a given RNA cluster is more dispersed throughout the cell. **B**, Polarization index and dispersion index demonstrated on a smFISH image. An RNA cluster with high PI and DI suggests that the RNA are found dispersed throughout the cell far away from the nucleus. An RNA cluster with low PI and DI suggests that the labeled RNA molecules are found to be highly concentrated at the perinuclear region. **C**, The workflow of Fiji macro-operation and data output.

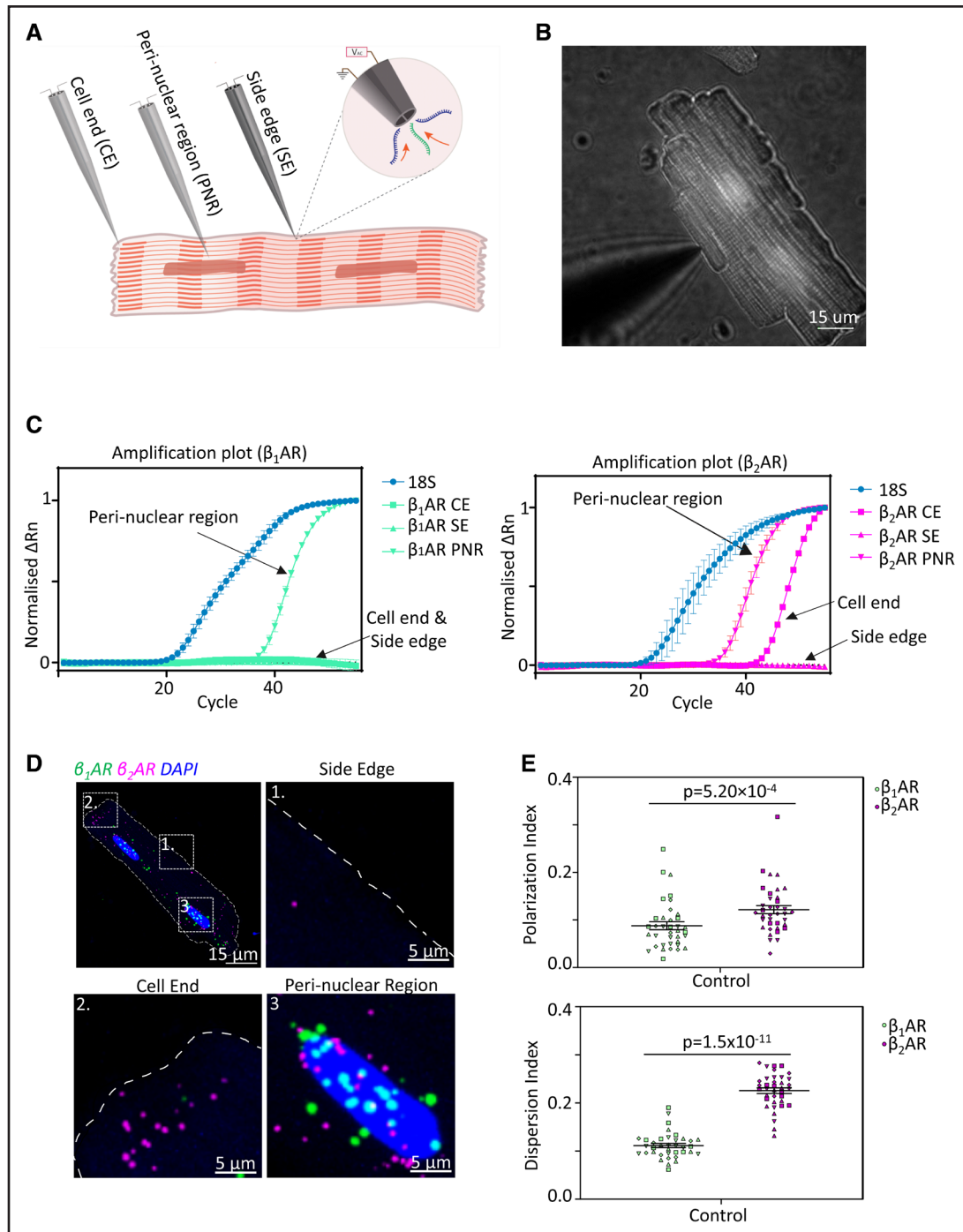


**Figure 2.**  $\beta_1$ AR (beta-1 adrenergic receptor) and  $\beta_2$ AR (beta-2 adrenergic receptor) mRNAs are differentially distributed in healthy cardiomyocytes.

**A**, A schematic of nanobiopsy procedure to obtain subcellular content using nanoscale tweezers. **B**, Microscopic image showing a control rat cardiomyocyte undergoing nanoscale biopsy. **C**, Representative reverse transcription-quantitative PCR (RT-qPCR) amplification plots of nanobiopsy extracted from different cellular compartments in healthy cardiomyocytes.  $\beta_1$ AR mRNA is mostly detected at the perinuclear region (PNR) but rarely at the cell ends (CE) and side edges (SE).  $\beta_2$ AR mRNAs are found near the nucleus and often closer to the plasma membrane compartments. 18S was used as housekeeping control and is detected in all nanobiopsy analyzed.  $N=5$ ,  $n \geq 15$ . **D**, RNAscope smFISH images showing  $\beta_1$ AR (green) and  $\beta_2$ AR (magenta) transcripts distribution in healthy cardiomyocytes.  $\beta_1$ AR mRNAs were found clustering around the perinuclear region, whereas  $\beta_2$ AR mRNAs are distributed throughout the cell (**E**) resulting in a higher polarization and dispersion index when compared with  $\beta_1$ -AR.  $N=4$ ,  $n=37$ . Data are represented as mean  $\pm$  SEM. Statistical significance was determined using the Wilcoxon matched-pairs signed rank test.

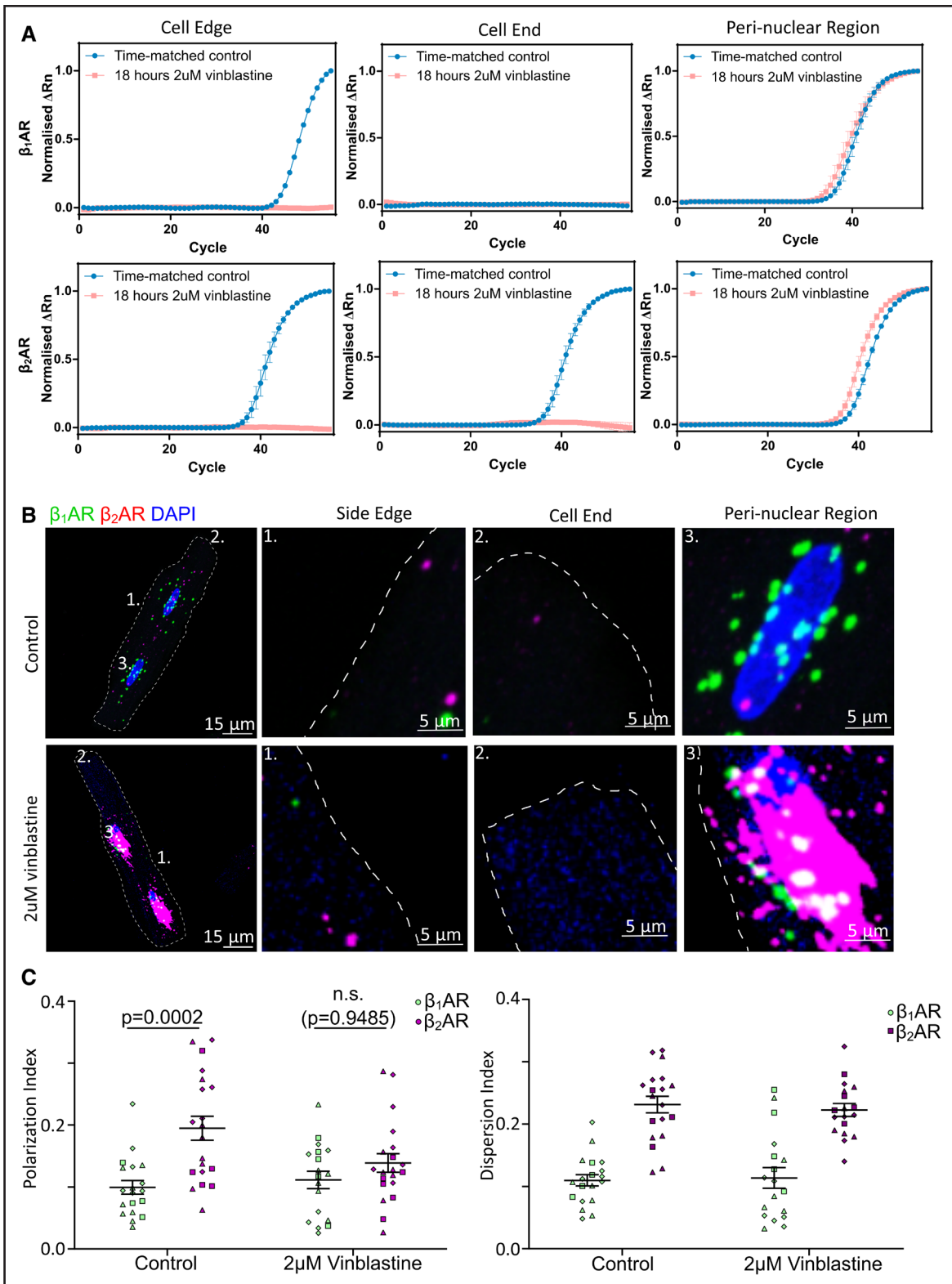


**Figure 3.  $\beta_2$ AR (beta-2 adrenergic receptor) mRNA transport in cardiomyocytes is microtubule dependent.**

**A**, When 2- $\mu$ M vinblastine was used to disrupt microtubules from cardiomyocytes,  $\beta_2$ AR became less likely to be detected close to the membrane but became more abundant around the nucleus, compared with a time-matched (18-hour incubation in culture) control. N=3, n $\geq$ 16. **B**, Representative RNAscope single molecule fluorescence in situ hybridization (smFISH) images showing that in 2- $\mu$ M vinblastine-treated cells and time-matched control,  $\beta_2$ AR (magenta) mRNAs are redistributed to the perinuclear region from the distal cytosol of the cell.  $\beta_1$ AR (beta-1 adrenergic receptor; green) mRNA, on the other hand, did not seem to be largely affected. **C**, Without an intact microtubule in cardiomyocytes, the differential localization of  $\beta_1$ AR and  $\beta_2$ AR transcripts was lost, and the difference in polarization between the 2 mRNAs of interest are no longer statistically significant. Data were represented as mean $\pm$ SEM. Statistical significance was determined using 2-way ANOVA with post hoc Tukey multiple comparisons test. N=3, n $\geq$ 18.

interest from control and vinblastine-treated ARVM. RT-qPCR analysis of the nanobiopsy samples showed that  $\beta_2$ AR mRNAs relocated from the cell periphery (side edges and cell ends) to the perinuclear region of ARVM after microtubule disruption (Figure 3A). Once again, the RT-qPCR results were validated using smFISH, which agreed with our qPCR findings. smFISH revealed that  $\beta_1$ AR-mRNA localization in vinblastine-treated cells was not statistically significant from control cells. However,  $\beta_2$ AR mRNAs were redistributed from the cell periphery to the perinuclear region, and differences in polarization between the 2 transcripts were lost, suggesting  $\beta_2$ AR-mRNA transportation was dependent on the microtubule network (Figure 3B and 3C).

Since 18 hours of 2  $\mu$ M vinblastine treatment has been found to have no statistically significant effect on  $\beta_1$ AR and  $\beta_2$ AR expression levels, we concluded that the changes we observed in  $\beta_2$ AR localization following microtubule disruption were a result of changes in physical redistribution of the mRNA molecules, but not due to altered gene expression. To control for drug-specific effect of vinblastine, the same smFISH experiment was performed on 10  $\mu$ M nocodazole-treated cells. In all these cases, a similar trend was observed where  $\beta_2$ AR mRNAs, but not  $\beta_1$ AR, trafficking in cardiomyocytes was affected by microtubule disruption (Figure S3).

### An Intact Microtubule Is Crucial for $\beta_2$ AR Trafficking, Translation, and Function

To investigate whether localization of the  $\beta$ -AR mRNAs to the cell periphery resulted in localized protein translation, we performed a single-cell RNA-protein co-detection assay to visualize the localization of  $\beta$ -AR mRNAs and their corresponding translated proteins in the same single isolated ARVM. The distance analysis has revealed that  $\beta_1$ AR mRNA molecules and their corresponding translated proteins almost always colocalize in the perinuclear region, but only in <40% in other parts of the cell. On the other hand,  $\beta_2$ AR mRNA molecules and their translated proteins colocalized at a much higher degree at >80% on average, regardless of the sub-compartments; in fact,  $\beta_2$ AR mRNAs tended to colocalize with its translated proteins more in the cytosol (89.9%) than in the perinuclear region (80.1%). This result suggests that  $\beta_2$ AR mRNA is much more likely to be locally translated into proteins compared with its  $\beta_1$ AR counterpart (Figure 4A and 4B).

We next studied if the newly synthesized  $\beta$ -AR proteins are located close to microtubules by immunostaining of  $\beta$ -tubulin and  $\beta$ -AR proteins. We analyzed the images using Mander coefficient, and it was found that  $\beta_2$ AR proteins indeed tended to colocalize with the microtubule network at a significantly higher degree as compared with  $\beta_1$ AR proteins, suggesting that  $\beta_2$ AR distribution relies on the microtubule network to a much higher degree than its  $\beta_1$ AR counterpart (Figure 4C and 4D).

To elucidate whether  $\beta_1$ AR and  $\beta_2$ AR mRNA localization and functional properties of their protein products depend on microtubules, we performed a Förster resonance energy transfer (FRET)-microscopy experiment by transducing cardiomyocytes with a plasma membrane-localized cAMP biosensor pmEpac2. We then stimulated  $\beta_1$ AR or  $\beta_2$ AR subtype-specific cAMP responses on the plasma membrane compartment in control and 2  $\mu$ M vinblastine-treated ARVMs. As expected, selective activation of  $\beta_1$ AR resulted in a substantial increase in cAMP production in both control and vinblastine-treated ARVM (Figure 4E). Differences in the FRET response between the control and vinblastine-treated group (Figure 4F) were not statistically significant, indicating that activation of cAMP synthesis by  $\beta_1$ AR receptors on the plasma membrane is independent of microtubules. However,  $\beta_2$ AR-specific cAMP response in vinblastine-treated cardiomyocytes was significantly lower than in control cells (Figure 4E and 4F), suggesting that microtubule disruption significantly impairs  $\beta_2$ AR receptor function on the plasma membrane. We therefore concluded that a microtubule-dependent mRNA trafficking mechanism governs the compartmentation/function of  $\beta_2$ AR but not  $\beta_1$ AR, on the plasma membrane. To control for the drug-specific effect of vinblastine, we also repeated the same FRET experiment on 10  $\mu$ M nocodazole-treated ARVMs, and we observed the same trend where  $\beta_2$ AR, but not  $\beta_1$ AR, receptor function was affected by microtubule disruption in cardiomyocytes (Figure S3).

To investigate if microtubule disruption would reduce the levels of  $\beta$ -AR, we quantified the amount of membrane-localized  $\beta_1$ AR and  $\beta_2$ AR proteins in control and vinblastine-treated cardiomyocytes after immunostaining. Interestingly, we found that the levels of both  $\beta_1$ AR and  $\beta_2$ AR localized to the plasma membrane were reduced at the edge of the cell following microtubule disruption (Figure 4F; Figure S4A). The distribution of both proteins was altered following vinblastine treatment, as both the density and regular distribution pattern of both  $\beta$ -AR subtype proteins were reduced (Figure S4A). To validate this result, a radioligand binding assay was performed to determine the ratio between  $\beta_1$ AR and  $\beta_2$ AR in control and vinblastine-treated cardiomyocytes. Analysis of the whole microsomal fraction containing all membrane compartments did not show any difference between treated and untreated cells in terms of  $\beta_2$ AR amounts (Figure S4A). However, strikingly, microtubule disruption led to a statistically significant reduction of the relative ratio of  $\beta_2$ AR/ $\beta_1$ ARs but almost no  $\beta_2$ AR binding detectable in the plasma membrane fraction, suggesting that the abovementioned changes in receptor localization may result from altered trafficking and distinct subcellular distribution in various membrane compartments (Figure S4B). On the contrary, actin depolymerization had no statistically significant effect on  $\beta_1$ AR or  $\beta_2$ AR protein localization or their function in the plasma membrane (Figure S7).



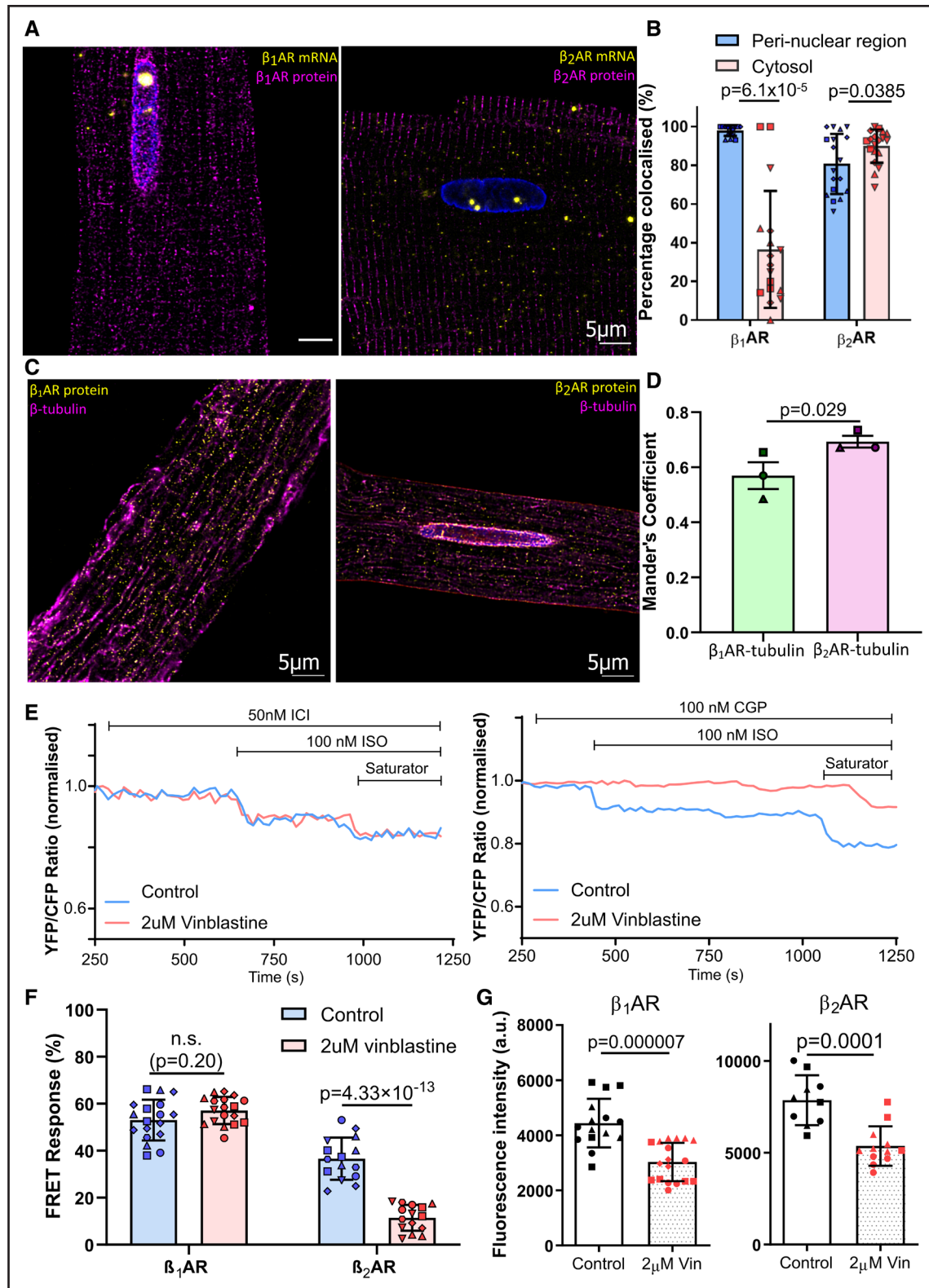


**Figure 4. An intact microtubule is crucial for  $\beta_2$ AR (beta-2 adrenergic receptor) trafficking, translation, and function.**

**A**, Representative fluorescent labeling of  $\beta_1$ AR (beta-1 adrenergic receptor) and  $\beta_2$ AR mRNA and their corresponding proteins. **B**, Quantification of mRNA protein co-detection shows that >90% of  $\beta_1$ AR mRNA colocalized with its protein at the perinuclear region, compared with <40% in the cytosol.  $\beta_2$ AR mRNA and protein tend to colocalize in the cytosol, further away from the nucleus. Colocalization was defined as the distance of a given RNA signal is <0.1  $\mu\text{m}$  from the closest corresponding protein signal. A detailed protocol can be found in the supplementary methodology. Magenta: proteins; yellow: RNA molecules.  $N \geq 3$ ,  $n \geq 17$ . Statistical significance was determined using Wilcoxon matched-pairs signed rank tests. **C**, Representative fluorescent labeling of either  $\beta_1$ AR or  $\beta_2$ AR protein and tubulin. **D**,  $\beta_2$ AR proteins colocalize with the microtubule (*Continued*)

## Both $\beta_1$ AR and $\beta_2$ AR Transcripts Are Redistributed in Failing Cardiomyocytes

After establishing differences in  $\beta_1$ AR and  $\beta_2$ AR mRNA localization, translation, and receptor function in healthy ARVMs, we next examined if their localization has changed in HF and whether redistribution of  $\beta_2$ AR proteins in failing cardiomyocytes, reported in one of our previous studies,<sup>16</sup> can be related to mislocalization of their mRNA.

We first performed smFISH on healthy and failing ARVMs. It was found that there was indeed redistribution of the 2 transcripts in failing cells compared with control (Figure 5A and 5B). Clustering analysis of the images showed that both  $\beta_1$ AR and  $\beta_2$ AR-mRNAs became more polarized and dispersed in failing ARVMs, indicating that both transcripts migrated further away from the nucleus and became less clustered.

Since hypertrophy is a common feature of failing cardiomyocytes, the clustering analysis results must be confirmed with a different technique, as the PI and DI were calculated based on the cell morphology. To address this, we performed a correlation analysis and found no statistically significant correlation between the cell area and the PI (Figure S5). Next, to confirm our smFISH analysis data, we analyzed nanoscale biopsies from the 3 cellular compartments of interest (perinuclear, cell end, and side edge) using TaqMan RT-qPCR. The results confirmed a redistribution of  $\beta_1$ AR and  $\beta_2$ AR mRNAs from the perinuclear region to cytosol close to the cell periphery in failing ARVM, consistent with the smFISH results (Figure 5C).

## T-Tubule Remodeling Contributes to $\beta_2$ AR Redistribution in HF

To elucidate the potential mechanism leading to  $\beta$ -AR mRNA redistribution in failing cardiomyocytes, we used a recently discovered detubulation agent, imipramine, to remove t-tubules from control cardiomyocytes, to investigate whether t-tubule remodeling, a known feature in failing cardiomyocytes, contributes to  $\beta$ -AR mRNA redistribution post-myocardial infarction.

After confirming the efficacy of 300  $\mu$ M imipramine in removing t-tubules from isolated ARVM (Figure S6), we

performed smFISH experiments on control and detubulated ARVMs (Figure 6A). Clustering analysis of smFISH images revealed that t-tubule remodeling does alter both  $\beta$ -AR mRNA localization patterns in cardiomyocytes. Both  $\beta_1$ AR and  $\beta_2$ AR mRNAs PI were increased (Figure 6B), an effect similar to that observed in failing cardiomyocytes. In terms of dispersion, only  $\beta_2$ AR transcripts' distribution was altered as the DI increased, in line with failing cardiomyocytes (Figure 6B). However, the dispersion pattern of  $\beta_1$ AR mRNAs was not statistically significant between control and detubulated ARVMs (Figure 6B), suggesting t-tubule remodeling affects  $\beta_2$ AR more statistically significantly than its  $\beta_1$ AR counterpart.

To test whether acute de-tubulation influences membrane  $\beta_2$ AR function and whether its effect is comparable to that of failing cardiomyocytes, we performed a FRET microscopy experiment using the membrane-localized FRET sensor pmEpac2, on both control, 300  $\mu$ M imipramine treated, and failing ARVMs. Unsurprisingly, de-tubulation significantly reduced  $\beta_2$ AR response on the cell membrane, similar to failing cardiomyocytes (Figure 6C). It should be pointed out that the total amount of cAMP available in the cell is not affected by de-tubulation treatment but is lower in failing cardiomyocytes (Figure 6C), and thus, the reduction in FRET response observed was due to altered  $\beta_2$ AR function on the membrane rather than changes to the total cAMP level available in the cell at that membrane compartment.

## DISCUSSION

In this study, we demonstrated that  $\beta_1$ AR and  $\beta_2$ AR-mRNAs are differentially localized in cardiomyocytes, suggesting possible differences in the membrane receptor trafficking mechanisms. We have also found that  $\beta_2$ AR, but not  $\beta_1$ AR, mRNA is transported in cardiomyocytes via the microtubule network. While previous studies<sup>27,28</sup> demonstrated that several cardiomyocyte mRNAs are locally translated into proteins, we have shown that not all mRNAs behave in this manner. This suggests that in ARVM, some, but not all, mRNAs are translated into proteins far from the nucleus, consistent with recent observations in murine cardiomyocytes.<sup>33</sup>

Various studies have demonstrated that compartmentation of  $\beta_2$ AR induces a cAMP response in ARVMs,<sup>40–44</sup>

**Figure 4 Continued.** network at a higher degree than their  $\beta_1$ AR counterpart, suggesting an intact microtubule is essential for  $\beta_2$ AR protein trafficking. N=3, n=12 to 21. Statistical significance was determined using a nested *t* test. **E**, Representative Förster resonance energy transfer (FRET) traces of  $\beta_1$ AR and  $\beta_2$ AR specific cAMP response in control and 2- $\mu$ M vinblastine-treated cardiomyocytes, normalized to baseline.  $\beta$ -AR subtype-specific blocker ( $\beta_1$ -blocker 100 nmol/L CGP 20712 **A**,  $\beta_2$ -blocker 50 nmol/L ICI-118 551) was added, and the nonselective  $\beta$ -agonist 100 nmol/L isoproterenol (ISO) was used to trigger  $\beta$ -AR subtype-specific response. A saturator (100  $\mu$ mol/L IBMX+10  $\mu$ mol/L forskolin) was then added to trigger maximum cAMP response of the cell. **F**,  $\beta_1$ AR- and  $\beta_2$ AR-specific cAMP response of control and 2  $\mu$ M vinblastine-treated cardiomyocytes, normalized to saturator response.  $\beta_2$ AR-specific cAMP response is significantly lower in microtubule-disrupted cardiomyocytes, whereas  $\beta_1$ AR-specific cAMP response was unaffected despite the absence of an intact microtubule network. Data were represented as mean $\pm$ SEM. N=6, n $\geq$ 15. Statistical significance was determined by 2-way ANOVA followed by post hoc Tukey multiple comparisons test. **G**, Quantification of immunofluorescent images of  $\beta_1$ AR and  $\beta_2$ AR in control and vinblastine-treated cardiomyocytes (representative fluorescent images are available in Figure S3). The amount of both  $\beta_1$ AR and  $\beta_2$ AR proteins on the cell surface was significantly reduced as the microtubule network was disrupted in cardiomyocytes. Statistical significance was determined by the Mann-Whitney *U* test ( $\beta_1$ AR) or the unpaired *t* test ( $\beta_2$ AR).

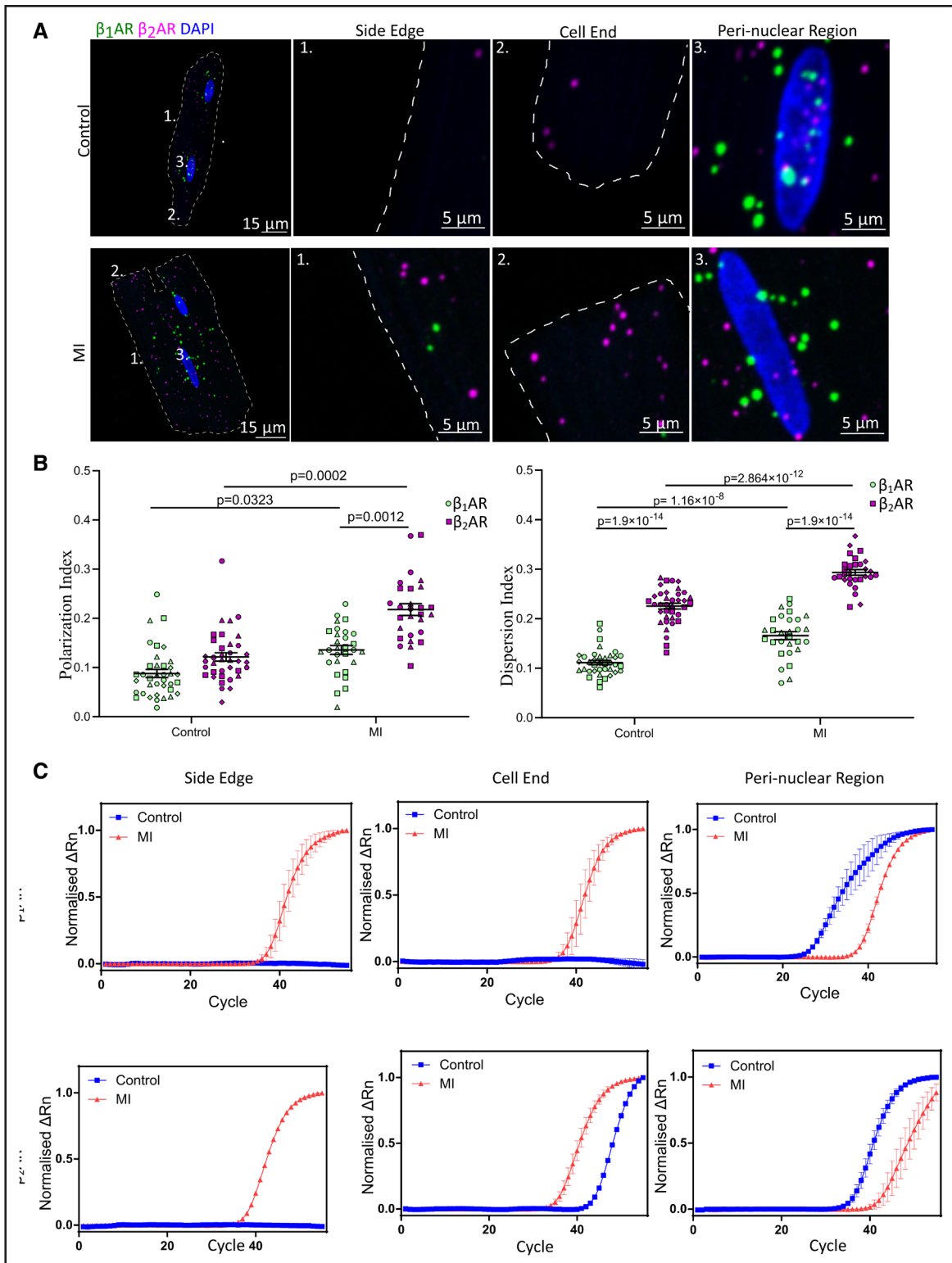


**Figure 5. Both  $\beta_1$ AR (beta-1 adrenergic receptor) and  $\beta_2$ AR (beta-2 adrenergic receptor) transcripts are redistributed in failing cardiomyocytes.**

**A**, Post-heart failure, both  $\beta_1$ AR and  $\beta_2$ AR mRNAs were found to have redistributed where they moved closer to the plasma membrane. **B**, The mRNA redistribution was reflected in the clustering analysis as an increase in both polarization index (PI) and dispersion index (DI) for both mRNAs of interest. Although both transcripts have redistributed post-myocardial infarction (MI), the differences between  $\beta_1$ AR and  $\beta_2$ AR persist.  $N \geq 3$ ,  $n = 29$ . Data are represented as mean  $\pm$  SEM. Statistical significances were determined using 2-way ANOVA with Sidak multiple comparisons test. **C**, Representative reverse transcription-quantitative PCR (RT-qPCR) amplification curves of nanobiopsy samples extracted from different cellular compartments confirm the changes in both  $\beta_1$ AR and  $\beta_2$ AR mRNA localization post-MI, where it became more likely to detect both  $\beta_1$ AR and  $\beta_2$ AR mRNA close to the cell membrane in failing cardiomyocytes.  $N = 5$ ,  $n \geq 15$ .

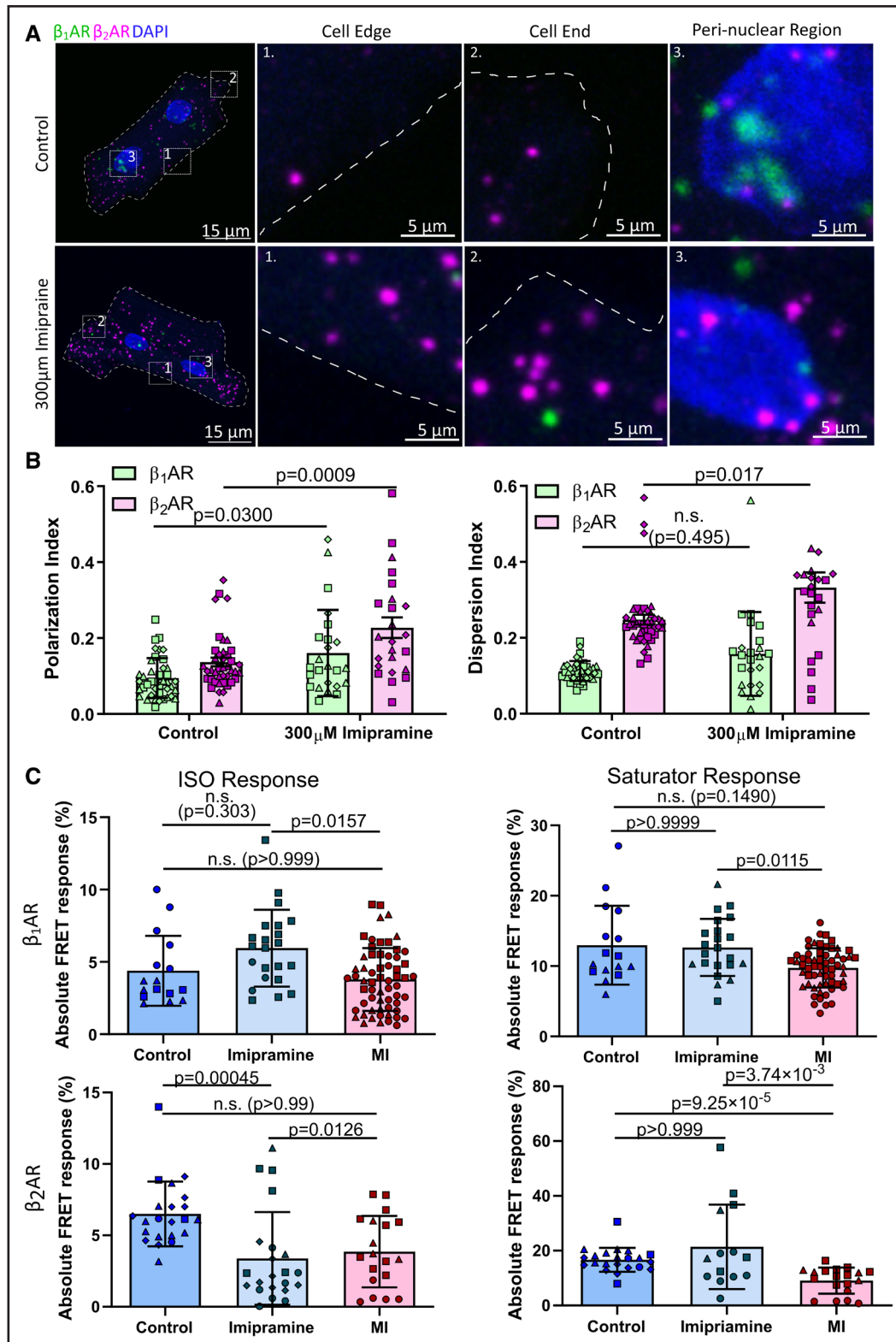


**Figure 6. Detubulation contributes to  $\beta_2$ AR (beta-2 adrenergic receptor) redistribution in heart failure.**

**A**, RNA scope smFISH images showing  $\beta_1$ AR (beta-1 adrenergic receptor) and  $\beta_2$ AR mRNA distribution in control and 300- $\mu$ M imipramine-treated, detubulated cardiomyocytes. **B**, Clustering analysis of single molecule fluorescence in situ hybridization (smFISH) images shows an increase in polarization index and dispersion index for  $\beta_2$ AR in detubulated myocytes. Polarization of  $\beta_1$ AR also significantly increased postdetubulation. N=3, n=24 to 41. Data were presented as mean $\pm$ SD. Statistical significance was determined using 2-way ANOVA with Šidák correction. **C**, Quantified absolute Förster resonance energy transfer (FRET) response (not normalized to saturator) shows imipramine-driven detubulation has a similar effect on  $\beta_2$ AR receptor function as myocardial infarction by reducing mainly  $\beta_2$ AR specific cyclic adenosine monophosphate (cAMP) output.  $\beta_1$ AR: N=3, n=16 to 61.  $\beta_2$ AR: N=3 to 4, n=19 to 22. Data were presented as mean $\pm$ SD. Statistical significance was determined using Kruskal-Wallis test.

and in 2010, one of our previous studies demonstrated the redistribution of functional  $\beta_2$ AR receptors on the plasma membrane and the loss of compartmentation; yet, the mechanism controlling this remained elusive at the time.<sup>16</sup> This study shows that, unlike  $\beta_1$ AR,  $\beta_2$ AR mRNA is localized throughout the whole cell. In addition, we found that  $\beta_2$ AR mRNA colocalized with its translated protein to a higher degree compared with  $\beta_1$ AR. We also found that, at the protein level,  $\beta_2$ AR showed a higher colocalization with the microtubule network than  $\beta_1$ AR. Taken together, this suggests that  $\beta_2$ AR is likely to be locally translated into functional receptors as shown for some other proteins.<sup>27,28</sup>

In neurons, where localized translation of protein is extensively studied, mRNA compartmentalization around the synapse and targeted, localized translation facilitate rapid physiological changes at the microdomains.<sup>25,26</sup> In the case of cardiomyocytes, however, this was not known to be the case. Although emerging evidence has suggested that various mRNAs are found throughout cardiomyocytes, and their transport is microtubule-dependent, our data have further demonstrated that some mRNAs, such as  $\beta_1$ AR and  $\beta_2$ AR differ in the way they are targeted for translation. The former could be mainly trafficked as translated proteins, whereas the latter could be translated in dedicated cellular compartments after the respective mRNA has been trafficked there. It is possible that these 2 functionally and structurally very similar receptors evolved to perform their function in different compartments by means of differential mRNA localization and subsequent translation of their products.

We are the first to show that mRNA molecules and mRNP destination sites are colocalized with the microtubules within the cell. This suggests that in cardiomyocytes, some mRNAs, such as  $\beta_2$ AR, are packaged into messenger ribonucleoproteins and are translated into proteins as they are transported to their final destination via microtubules. This idea is supported by a previous study, where the authors found that the protein synthesis machinery, namely the Golgi apparatus and endoplasmic reticulum, is scattered throughout a cardiomyocyte.<sup>33</sup> In the same study, the authors also revealed that in cardiomyocytes, ribosome-associated mRNAs are distributed throughout the cell. They activated the mTOR pathway to increase transcription and protein synthesis. It was found that by doing so, there was a global increase of ribosome-associated mRNAs throughout the cell without any changes in their distribution.<sup>33</sup> This finding further supports the idea that cardiomyocyte mRNAs may be translated into functional proteins as they are being transported along the microtubule network toward their final destination.

Our FRET data provided additional evidence supporting this idea. Depolymerization of microtubules caused a significant downregulation of  $\beta_2$ AR-induced cAMP release on the plasma membrane, whereas the

$\beta_1$ AR receptor function was not statistically significantly affected, indicating there is a downregulation in  $\beta_2$ AR but not  $\beta_1$ AR receptor number on the cell surface when microtubules are disrupted. We have also found that neither  $\beta_{1/2}$ AR protein localization pattern nor their function on the membrane compartments were regulated by the actin network, which explains why the presence of actin depolymerizing agent cytochalasin D did not affect  $\beta$ -adrenergic mediated cAMP response at multiple subcellular nanodomains in cardiomyocytes.<sup>45</sup> Our study focused predominantly on mechanisms regulating membrane localization of  $\beta_1$ AR and  $\beta_2$ AR in cardiomyocytes. The role of microtubules in redistributing these proteins to other cellular compartments is beyond the scope of this study and will require further investigation.

In failing cardiomyocytes,  $\beta_1$ AR and  $\beta_2$ AR-mRNAs became more polarized (having traveled further away from the nucleus) and more dispersed (less clustered in relation to each other). We have also noticed that acute de-tubulation using imipramine led to  $\beta_2$ AR mRNA redistribution, a pattern that was also observed in failing cardiomyocytes. To investigate whether acute de-tubulation in healthy cardiomyocytes could alter the amount of functional  $\beta_2$ AR proteins in the plasma membrane, we performed FRET microscopy on healthy, detubulated, and failing cardiomyocytes. The results show that detubulation indeed had a similar effect as myocardial infarction on membrane-localized  $\beta_2$ AR at a functional level. The results suggest that t-tubule remodeling is likely to have contributed to the redistribution of the  $\beta_2$ AR mRNA, hence a physical redistribution of the translated proteins and altered  $\beta$ -AR mediated cAMP signaling pathway in failing ARVMs. A 2014 study has revealed the link between microtubule densification in failing hearts leading to t-tubule remodeling in pressure-overloaded murine hearts due to a defective transport of junctophilin2, a protein that anchors the t-tubules to the sarcoplasmic reticulum membranes.<sup>36</sup> It is, therefore, likely that in failing hearts, there is the densification of the microtubule network in cardiomyocytes, leading to insufficient or defective transport of proteins toward the cell periphery. This leads to t-tubule remodeling and subsequent redistribution of  $\beta$ -AR mRNAs and proteins, causing the loss of compartmentation of  $\beta_2$ AR-mediated cAMP signaling.<sup>16</sup>  $\beta_2$ AR then became predominantly associated with the stimulatory G-protein and further drives pathological phenotype in a positive feedback loop. This may be even more exacerbated by the remodeling of the phosphodiesterases.<sup>46</sup>

To conclude, differential  $\beta_1$ AR and  $\beta_2$ AR localization in healthy cardiomyocytes are dependent on the asymmetrical microtubule-dependent trafficking of mRNA (for  $\beta_2$ AR) for or protein (for  $\beta_1$ AR), underlying the distinctive compartmentation of the 2 beta-adrenergic receptors on the plasma membrane. Following myocardial infarction, the localization pattern of beta-adrenergic receptor

alters, partly due to the t-tubule remodeling and microtubule restructuring, eventually leading to distorted  $\beta$ 2AR-mediated cAMP signaling.

## ARTICLE INFORMATION

Received June 2, 2023; revision received October 11, 2023; accepted October 11, 2023.

### Affiliations

National Heart and Lung Institute (Z.K., S.M., A.L., K.S.A., J.C., I.K., J.F., J.L.S.-A., C.A.M., P.S., B.W.-S., P.T.W., J.G.) and Department of Chemistry (Z.K., B.P.N., A.P.I., J.B.E.), Imperial College London, United Kingdom. Department of Pure and Applied Chemistry, University of Strathclyde, United Kingdom (B.P.N.). Sir William Dunn School of Pathology, University of Oxford, United Kingdom (M.M.L.). Division of Cancer and Stem Cells, University of Nottingham Biodiscovery Institute, United Kingdom (A.K.). Gene Regulation and RNA Biology, School of Pharmacy, University of Nottingham, United Kingdom (A.K.). FILM Facility, Imperial College London, United Kingdom (S.R.). Institute of Experimental Cardiovascular Research, University Medical Center, Hamburg-Eppendorf, Germany (H.S., V.O.N.). School of Life and Health Sciences, University of Roehampton, United Kingdom (P.T.W.).

### Acknowledgments

The authors thank the Facility for Imaging by Light Microscopy and the Center of Excellence Cellular Mechanosensing and Functional Microscopy at Imperial College London.

### Sources of Funding

This work was supported by the British Heart Foundation grant (RG/F/22/110081 to J. Gorelik/J.L. S.-A.), A.P. Ivanov and J.B. Edel acknowledge support from EP-SRC grants EP/P011985/1, EP/V049070/1, and Analytical Chemistry Trust Fund grant 600322/05. This project has also received funding from the European Research Council (ERC) under the European Union's Horizon 2020 research and innovation program (grant agreement nos. 724300 and 875525). B. Wojciak-Stothard acknowledges BHF grant PG/19/19/34286. B.P. Nadapuram acknowledges support from the Analytical Chemistry Trust Fund and Community for Analytical Measurement Science fellowship (Ref. No. 600310/21/07).

### Disclosures

None.

### Supplemental Material

Expanded Material and Methods

References 47–53

Figures S1–S7

Supplementary Scripts

Data and Statistics

Major Resource Table

## REFERENCES

- Savarese G, Lund LH. Global public health burden of heart failure. *Card Fail Rev*. 2017;3:7–11. doi: 10.15420/cfr.2016:25:2
- Ziaeian B, Fonarow GC. Epidemiology and aetiology of heart failure. *Nat Rev Cardiol*. 2016;13:368–378. doi: 10.1038/nrcardio.2016.25
- Brodde O-E. Beta-adrenoceptors in cardiac disease. *Pharmacol Ther*. 1993;60:405–430. doi: 10.1016/0163-7258(93)90030-h
- Brodde O-E, Michel MC. Adrenergic and muscarinic receptors in the human heart. *Pharmacol Rev*. 1999;51:651–690.
- Gauthier C, Langin D, Balligand J-L.  $\beta$ 3-Adrenoceptors in the cardiovascular system. *Trends Pharmacol Sci*. 2000;21:426–431. doi: 10.1016/s0165-6147(00)01562-5
- Heubach JF, Rau T, Eschenhagen T, Ravens U, Kaumann AJ. Physiological antagonism between ventricular  $\beta$ 1-adrenoceptors and  $\alpha$ 1-adrenoceptors but no evidence for  $\beta$ 2- and  $\beta$ 3-adrenoceptor function in murine heart. *Br J Pharmacol*. 2002;136:217–229. doi: 10.1038/sj.bjp.0704700
- Devic E, Xiang Y, Gould D, Kobilka B.  $\beta$ -adrenergic receptor subtype-specific signaling in cardiac myocytes from  $\beta$ 1 and  $\beta$ 2 adrenoceptor knockout mice. *Mol Pharmacol*. 2001;60:577–583.
- Kohout TA, Takaoka H, McDonald PH, Perry SJ, Mao L, Lefkowitz RJ, Rockman HA. Augmentation of cardiac contractility mediated by the human  $\beta$ 3-adrenergic receptor overexpressed in the hearts of transgenic mice. *Circulation*. 2001;104:2485–2491. doi: 10.1161/hc4501.098933
- Rockman HA, Koch WJ, Lefkowitz RJ. Seven-transmembrane-spanning receptors and heart function. *Nature*. 2002;415:206–212. doi: 10.1038/415206a
- Xiang Y, Kobilka BK. Myocyte adrenoceptor signaling pathways. *Science*. 2003;300:1530–1532. doi: 10.1126/science.1079206
- Xiao R-P, Zhu W, Zheng M, Chakir K, Bond R, Lakatta EG, Cheng H. Subtype-specific  $\beta$ -adrenoceptor signaling pathways in the heart and their potential clinical implications. *Trends Pharmacol Sci*. 2004;25:358–365. doi: 10.1016/j.tips.2004.05.007
- Bristow MR, Ginsburg R, Umans V, Fowler M, Minobe W, Rasmussen R, Zera P, Menlove R, Shah P, Jamieson S. Beta 1- and beta 2-adrenergic-receptor subpopulations in nonfailing and failing human ventricular myocardium: coupling of both receptor subtypes to muscle contraction and selective beta 1-receptor down-regulation in heart failure. *Circ Res*. 1986;59:297–309. doi: 10.1161/01.RES.59.3.297
- Ungerer M, Böhm M, Elce JS, Erdmann E, Lohse MJ. Altered expression of beta-adrenergic receptor kinase and beta 1-adrenergic receptors in the failing human heart. *Circulation*. 1993;87:454–463. doi: 10.1161/01.CIR.87.2.454
- Kiuchi K, Shannon RP, Komamura K, Cohen DJ, Bianchi C, Homcy CJ, Vatner SF, Vatner DE. Myocardial beta-adrenergic receptor function during the development of pacing-induced heart failure. *J Clin Invest*. 1993;91:907–914. doi: 10.1172/JCI116312
- Nikolaev VO, Bünemann M, Schmittecker E, Lohse MJ, Engelhardt S. Cyclic AMP imaging in adult cardiac myocytes reveals far-reaching  $\beta$ 1-adrenergic but locally confined  $\beta$ 2-adrenergic receptor-mediated signaling. *Circ Res*. 2006;99:1084–1091. doi: 10.1161/01.RES.0000250046.69918.d5
- Nikolaev VO, Moshkov A, Lyon AR, Miragoli M, Novak P, Paur H, Lohse MJ, Korchev YE, Harding SE, Gorelik J.  $\beta$ 2-adrenergic receptor redistribution in heart failure changes cAMP compartmentation. *Science*. 2010;327:1653–1657. doi: 10.1126/science.1185988
- Chen B, Li Y, Jiang S, Xie Y-P, Guo A, Kutschke W, Zimmerman K, Weiss RM, Miller FJ, Anderson ME, et al.  $\beta$ -Adrenergic receptor antagonists ameliorate myocyte T-tubule remodeling following myocardial infarction. *FASEB J*. 2012;26:2531–2537. doi: 10.1096/fj.11-199505
- Courelli V, Uchida K, Vite A, Prosser B, Margulies KB, Ibrahim M. Roles of mechanical overload and the microtubule network in mediating T-tubule remodeling. *Circulation*. 2022;146:A11506–A11506. doi: 10.1161/circ.146.suppl\_1.11506
- Ibrahim M, Gorelik J, Yacoub MH, Terracciano CM. The structure and function of cardiac t-tubules in health and disease. *Proc Biol Sci*. 2011;278:2714–2723. doi: 10.1098/rspb.2011.0624
- Lyon AR, MacLeod KT, Zhang Y, Garcia E, Kanda GK, Lab MJ, Korchev YE, Harding SE, Gorelik J. Loss of T-tubules and other changes to surface topography in ventricular myocytes from failing human and rat heart. *Proc Natl Acad Sci USA*. 2009;106:6854–6859. doi: 10.1073/pnas.0809777106
- Setterberg IE, Le C, Frisk M, Perdreau-Dahl H, Li J, Louch WE. The physiology and pathophysiology of T-tubules in the heart. *Front Physiol*. 2021;12:718404. doi: 10.3389/fphys.2021.718404
- Wei S, Guo A, Chen B, Kutschke W, Xie Y-P, Zimmerman K, Weiss RM, Anderson ME, Cheng H, Song L-S. T-tubule remodeling during transition from hypertrophy to heart failure. *Circ Res*. 2010;107:520–531. doi: 10.1161/CIRCRESAHA.109.212324
- Parola AL, Kobilka BK. The peptide product of a 5' leader cistron in the beta 2 adrenergic receptor mRNA inhibits receptor synthesis. *J Biol Chem*. 1994;269:4497–4505. doi: 10.1016/s0021-9258(17)41806-0
- Tholanikunnel BG, Joseph K, Kandasamy K, Baldys A, Raymond JR, Luttrell LM, McDermott PJ, Fernandes DJ. Novel mechanisms in the regulation of G protein-coupled receptor trafficking to the plasma membrane. *J Biol Chem*. 2010;285:33816–33825. doi: 10.1074/jbc.M110.168229
- Shigeoka T, Jung H, Jung J, Turner-Bridger B, Ohk J, Lin JQ, Amieux PS, Holt CE. Dynamic axonal translation in developing and mature visual circuits. *Cell*. 2016;166:181–192. doi: 10.1016/j.cell.2016.05.029
- Lyles V, Zhao Y, Martin KC. Synapse formation and mRNA localization in cultured Aplysia neurons. *Neuron*. 2006;49:349–356. doi: 10.1016/j.neuron.2005.12.029
- Lewis YE, Moskovitz A, Mutlak M, Heineke J, Caspi LH, Kehat I. Localization of transcripts, translation, and degradation for spatio-temporal sarcomere maintenance. *J Mol Cell Cardiol*. 2018;116:16–28. doi: 10.1016/j.yjmcc.2018.01.012
- Scarborough EA, Uchida K, Vogel M, Ertlitzki N, Iyer M, Phyto SA, Bogush A, Kehat I, Prosser BL. Microtubules orchestrate local

- translation to enable cardiac growth. *Nat Commun.* 2021;12:1547. doi: 10.1038/s41467-021-21685-4
29. Hendricks AG, Perlson E, Ross JL, Schroeder HW, Tokito M, Holzbaur EL. Motor coordination via a tug-of-war mechanism drives bidirectional vesicle transport. *Curr Biol.* 2010;20:697–702. doi: 10.1016/j.cub.2010.02.058
  30. Delanoue R, Davis I. Dynein anchors its mRNA cargo after apical transport in the *Drosophila* blastoderm embryo. *Cell.* 2005;122:97–106. doi: 10.1016/j.cell.2005.04.033
  31. Encalada SE, Szpankowski L, Xia C-h, Goldstein LS. Stable kinesin and dynein assemblies drive the axonal transport of mammalian prion protein vesicles. *Cell.* 2011;144:551–565. doi: 10.1016/j.cell.2011.01.021
  32. Rai AK, Rai A, Ramaiya AJ, Jha R, Mallik R. Molecular adaptations allow dynein to generate large collective forces inside cells. *Cell.* 2013;152:172–182. doi: 10.1016/j.cell.2012.11.044
  33. Bogdanov V, Soltisz AM, Moise N, Sakuta G, Orengo BH, Janssen PM, Weinberg SH, Davis JP, Veerarraghavan R, Györke S. Distributed synthesis of sarcolemmal and sarcoplasmic reticulum membrane proteins in cardiac myocytes. *Basic Res Cardiol.* 2021;116:1–16.
  34. Mitchison T, Kirschner M. Dynamic instability of microtubule growth. *Nature.* 1984;312:237–242. doi: 10.1038/312237a0
  35. Prins KW, Asp ML, Zhang H, Wang W, Metzger JM. Microtubule-mediated misregulation of junctophilin-2 underlies T-tubule disruptions and calcium mishandling in mdx mice. *JACC Basic Transl Sci.* 2016;1:122–130. doi: 10.1016/j.jacbs.2016.02.002
  36. Zhang C, Chen B, Guo A, Zhu Y, Miller JD, Gao S, Yuan C, Kutschke W, Zimmerman K, Weiss RM, et al. Microtubule-mediated defects in junctophilin-2 trafficking contribute to myocyte transverse-tubule remodeling and Ca<sup>2+</sup> handling dysfunction in heart failure. *Circulation.* 2014;129:1742–1750. doi: 10.1161/CIRCULATIONAHA.113.008452
  37. Guo A, Zhang X, Iyer VR, Chen B, Zhang C, Kutschke WJ, Weiss RM, Franzini-Armstrong C, Song L-S. Overexpression of junctophilin-2 does not enhance baseline function but attenuates heart failure development after cardiac stress. *Proc Natl Acad Sci USA.* 2014;111:12240–12245. doi: 10.1073/pnas.1412729111
  38. Stueland M, Wang T, Park HY, Mili S. RDI calculator: an analysis tool to assess RNA distributions in cells. *Sci Rep.* 2019;9:8267. doi: 10.1038/s41598-019-44783-2
  39. Nadappuram BP, Cadinu P, Barik A, Ainscough AJ, Devine MJ, Kang M, Gonzalez-Garcia J, Kittler JT, Willison KR, Vilar R, et al. Nanoscale tweezers for single-cell biopsies. *Nat Nanotechnol.* 2019;14:80–88. doi: 10.1038/s41565-018-0315-8
  40. Bastug-Özel Z, Wright PT, Kraft AE, Pavlovic D, Howie J, Froese A, Fuller W, Gorelik J, Shattock MJ, Nikolaev VO. Heart failure leads to altered  $\beta$ 2-adrenoceptor/cyclic adenosine monophosphate dynamics in the sarcolemmal phospholemman/Na<sup>+</sup> K ATPase microdomain. *Cardiovasc Res.* 2019;115:546–555. doi: 10.1093/cvr/cvy221
  41. Berisha F, Götz KR, Wegener JW, Brandenburg S, Subramanian H, Molina CE, Ruffer A, Petersen J, Bernhardt A, Girdauskas E, et al. cAMP imaging at ryanodine receptors reveals  $\beta$ 2-adrenoceptor driven arrhythmias. *Circ Res.* 2021;129:81–94. doi: 10.1161/CIRCRESAHA.120.318234
  42. MacDougall DA, Agarwal SR, Stopford EA, Chu H, Collins JA, Longster AL, Colyer J, Harvey RD, Calaghan S. Caveolae compartmentalise  $\beta$ 2-adrenoceptor signals by curtailing cAMP production and maintaining phosphatase activity in the sarcoplasmic reticulum of the adult ventricular myocyte. *J Mol Cell Cardiol.* 2012;52:388–400. doi: 10.1016/j.yjmcc.2011.06.014
  43. Rudokas MW, Post JP, Sataray-Rodriguez A, Sherpa RT, Moshal KS, Agarwal SR, Harvey RD. Compartmentation of  $\beta$ 2-adrenoceptor stimulated cAMP responses by phosphodiesterase types 2 and 3 in cardiac ventricular myocytes. *Br J Pharmacol.* 2021;178:1574–1587. doi: 10.1111/bph.15382
  44. Wright PT, Nikolaev VO, O'Hara T, Diakonov I, Bhargava A, Tokar S, Schobesberger S, Shevchuk AI, Sikkil MB, Wilkinson R, et al. Caveolin-3 regulates compartmentation of cardiomyocyte  $\beta$ 2-adrenergic receptor-mediated cAMP signaling. *J Mol Cell Cardiol.* 2014;67:38–48. doi: 10.1016/j.yjmcc.2013.12.003
  45. Surdo NC, Berrera M, Koschinski A, Brescia M, Machado MR, Carr C, Wright P, Gorelik J, Morotti S, Grandi E, et al. FRET biosensor uncovers cAMP nano-domains at  $\beta$ -adrenergic targets that dictate precise tuning of cardiac contractility. *Nat Commun.* 2017;8:15031. doi: 10.1038/ncomms15031
  46. Schobesberger S, Wright P, Tokar S, Bhargava A, Mansfield C, Glukhov AV, Poulet C, Buzuk A, Monzpart A, Sikkil M, et al. T-tubule remodelling disturbs localized  $\beta$ 2-adrenergic signalling in rat ventricular myocytes during the progression of heart failure. *Cardiovasc Res.* 2017;113:770–782. doi: 10.1093/cvr/cvx074
  47. Lewis CJ, Gong H, Brown MJ, Harding SE. Overexpression of  $\beta$ 1-adrenoceptors in adult rat ventricular myocytes enhances CGP 12177A cardiostimulation: implications for "putative" $\beta$ 4-adrenoceptor pharmacology. *Br J Pharmacol.* 2004;141:813–824. doi: 10.1038/sj.bjp.0705668
  48. Bourcier A, Barthe M, Bedioune I, Lechêne P, Miled HB, Vandecasteele G, Fischmeister R, Leroy J. Imipramine as an alternative to formamide to detubulate rat ventricular cardiomyocytes. *Exp Physiol.* 2019;104:1237–1249. doi: 10.1113/EP087760
  49. Park HY, Trcek T, Wells AL, Chao JA, Singer RH. An unbiased analysis method to quantify mRNA localization reveals its correlation with cell motility. *Cell Rep.* 2012;1:179–184. doi: 10.1016/j.celrep.2011.12.009
  50. Medvedev RY, Sanchez-Alonso JL, Mansfield CA, Judina A, Francis AJ, Pagiatakis C, Trayanova N, Glukhov AV, Miragoli M, Faggian G, et al. Local hyperactivation of L-type Ca<sup>2+</sup> channels increases spontaneous Ca<sup>2+</sup> release activity and cellular hypertrophy in right ventricular myocytes from heart failure rats. *Sci Rep.* 2021;11:4840. doi: 10.1038/s41598-021-84275-w
  51. Ramuz M, Hasan A, Gruscheski L, Diakonov I, Pavlaki N, Nikolaev VO, Harding S, Dunsby C, Gorelik J. A software tool for high-throughput real-time measurement of intensity-based ratio-metric FRET. *Cells.* 2019;8:1541. doi: 10.3390/cells8121541
  52. Wachten S, Masada N, Ayling L-J, Ciruela A, Nikolaev VO, Lohse MJ, Cooper DM. Distinct pools of cAMP centre on different isoforms of adenylyl cyclase in pituitary-derived GH3B6 cells. *J Cell Sci.* 2010;123:95–106. doi: 10.1242/jcs.058594
  53. Paur H, Wright PT, Sikkil MB, Tranter MH, Mansfield C, O'gara P, Stuckey DJ, Nikolaev VO, Diakonov I, Pannell L, et al. High levels of circulating epinephrine trigger apical cardiodepression in a  $\beta$ 2-adrenergic receptor/Gi-dependent manner: a new model of Takotsubo cardiomyopathy. *Circulation.* 2012;126:697–706. doi: 10.1161/CIRCULATIONAHA.112.111591